

# Synergism between particle-based multiplexing and microfluidics technologies may bring diagnostics closer to the patient

S. Derveaux · B. G. Stubbe · K. Braeckmans ·  
C. Roelant · K. Sato · J. Demeester · S. C. De Smedt

Received: 3 December 2007 / Revised: 4 February 2008 / Accepted: 6 March 2008 / Published online: 6 May 2008  
© Springer-Verlag 2008

**Abstract** In the field of medical diagnostics there is a growing need for inexpensive, accurate, and quick high-throughput assays. On the one hand, recent progress in microfluidics technologies is expected to strongly support the development of miniaturized analytical devices, which will speed up (bio)analytical assays. On the other hand, a higher throughput can be obtained by the simultaneous screening of one sample for multiple targets (multiplexing) by means of encoded particle-based assays. Multiplexing at the macro level is now common in research labs and is expected to become part of clinical diagnostics. This review aims to debate on the “added value” we can expect from (bio)analysis with particles in microfluidic devices. Technologies to (a) decode, (b) analyze, and (c) manipulate the particles are described. Special emphasis is placed on the challenges of integrating currently existing detection platforms for encoded microparticles into microdevices and on

promising microtechnologies that could be used to down-scale the detection units in order to obtain compact miniaturized particle-based multiplexing platforms.

**Keywords** Bioassays · Biochips/high-throughput screening · Microfluidics/microfabrication · Encoded particles · Multiplexing · Integrated systems

## Introduction

Many automated systems have been introduced in the field of medical diagnostics to enable more rapid and efficient data collection from the incredible amount of samples that hospitals deal with daily. However, such automated equipment is mostly not suitable for use in small diagnostic and research laboratories and for decentralized point-of-care testing, as they require highly qualified personnel, are often not portable and/or are too expensive. Hence, there is an increasing need for (a) accurate, (b) quick, (c) miniaturized, and (d) cheap innovative tools which should bring medical diagnostics closer to the patient.

There is no doubt that the recent progress in microfluidics technologies will strongly support the development of miniaturized analytical devices [1]. Microfluidics involves the manipulation, transport and analysis of fluids in micrometer-sized channels. A “liquid microspace” has characteristic features which differ from the properties of a “liquid bulk”: high interface-to-volume ratio, small heat capacity and, especially, short diffusion distances. The latter is a useful property in analysis, because the time a molecule needs to diffuse from point a to point b is proportional to the square of the distance between a and b [2]; While it takes several hours to overcome 1 cm, it only takes tens of seconds to overcome 100  $\mu\text{m}$ .

---

S. Derveaux and B. G. Stubbe contributed equally to this work.

---

S. Derveaux · B. G. Stubbe · K. Braeckmans · J. Demeester ·  
S. C. De Smedt (✉)  
Laboratory of General Biochemistry and Physical Pharmacy,  
Department of Pharmaceutics, Ghent University,  
Harelbekestraat 72,  
9000 Ghent, Belgium  
e-mail: Stefaan.Desmedt@Ugent.be

C. Roelant  
Memobead Technologies NV,  
Rupelweg 10,  
2850 Boom, Belgium

K. Sato  
Department of Applied Chemistry, School of Engineering,  
The University of Tokyo,  
7-3-1 Hongo, Bunkyo-Ku,  
Tokyo 113-8656, Japan

The microfluidic concept has already evolved into promising analytical “lab-on-a-chip” (LOC) tools [3]. The LOC concept, or the “micro total analysis system” ( $\mu$ TAS) as it is today commonly referred to, was proposed in the early 1990s by Manz et al. [4]. Since that time, the field has bloomed and branched off into many areas with different applications, such as single molecule analysis [5], single cell processing and analysis [6], biological and chemical analysis [7–14], point of care testing [15, 16], clinical and forensic analysis [17], molecular and medical diagnostics [18–21], combinatorial chemistry [22] and drug discovery [23]. The fact that LOC systems are compact, which allows the automation of complex tasks, makes them very attractive [24].

A higher throughput in (bio)analysis can be obtained (a) by the parallel screening of multiple samples for one target, (b) by the simultaneous screening of one sample for multiple targets (multiplexing), or (c) by a combination of both, as recently reviewed by Situma et al. [25]. In microfluidics, a higher throughput is currently obtained by the parallel screening of a number of samples in a number of channels in one device. Sato et al. [26] fabricated a device with branching multichannels that allows four samples to be processed simultaneously. The assay time for four samples was 50 minutes, instead of 35 min for one sample in a single-channel assay. Another way to realize higher throughput analysis in microfluidic devices is by multiplexing, i.e., the simultaneous detection of multiple analytes in a sample present in one channel. Kartalov et al. reported a multi-antigen microfluidic fluorescence immunoassay which measures up to five analytes for each of ten samples in a 100-chamber polydimethylsiloxane (PDMS) microchip [27]. Multiplexing at the “macro” level is now common in research labs and is expected to become part of clinical diagnostics [28–30]. Both “planar arrays” (often called “microarrays”) and “suspension arrays” (particle-based arrays) have been developed for multiplexing purposes.

Because microarrays allow (ultra)high density analysis of samples, they have become standard tools for gene expression analysis [31]. Multiplexing necessitates an encoding scheme for molecular identification; the code allows the capture probe bound at a particular position on the array to be identified, and so it is also possible to know which analyte is analyzed. Whereas planar arrays strictly rely on spatial positional encoding, particle-based arrays have used a great number of encoding schemes that can be classified as optical, graphical, electronic or physical [32, 33]. Particle-based arrays benefit from (a) “near-solution” kinetics, which means that the kinetics between a molecule bound to the surface of a particle and a free molecule equals those between two free molecules, (b) lower instrument-related costs, (c) higher sample throughput, and (d) good

quality control by batch synthesis [34, 35]. When compared with microarrays, particle-based arrays offer a more flexible choice of the “probe set;” the detection of extra targets only implies the addition of extra microparticles to the sample, while a new microarray has to be made in the case of microarray-assaying. Particle-based arrays are especially favorable compared to microarrays when a modest rather than a very high number of targets must be analyzed simultaneously. This feature may explain the recent exponential increase in particle-based applications at the “macro” level [28].

Currently, multiplexing at the microlevel is mainly done by combining flat surface microarrays with microchannels. Delehanty and Ligler [36] used noncontact microarray printing to immobilize biotinylated capture antibodies at discrete locations on an avidin-coated microscope slide and processed the samples with a six-channel flow module. Assays were completed in 15 min. The group of Delamarche combined concepts of micromosaic immunoassays and microfluidic networks to detect C-reactive protein (CRP) and other cardiac markers [37, 38]. By using  $20\ \mu\text{m} \times 10\ \mu\text{m}$  channels (5 mm in length), CRP was detected in ten minutes in only one microliter of human plasma down to concentrations of 30 ng/ml. So far only a few examples have been reported of multiplexing by particles in microfluidic devices [39]. One of the problems is that the implementation of the detection systems currently used to analyze particles in macro-assays into microfluidic devices is not straightforward.

This review discusses the “added value” we can expect from (bio)analysis with particles in microfluidic devices. Technologies to (a) decode, (b) analyze and (c) manipulate the particles are described. Also, an interdisciplinary effort is made to overview possibilities for the integration of different processes, like decoding and sorting of encoded particles.

### Strategies to decode particles

Clearly, to achieve multiplexing with particles in microfluidic devices, one should be able to decode the positive particles. In macro assays with encoded particles, three decoding platforms are generally used: flow (cyto)meter platforms, optical reading platforms, and fibre optic platforms. Although some well-written reviews have been published on this matter [32, 33, 40, 41], the next section provides a brief overview.

#### Flow (cyto)meter platform

One way to optically encode particles is by attaching chromophores, fluorophores or quantum dots to the surface,

or by incorporating one or more fluorescent dyes inside the particles. The code is based on the spectrum and/or the intensity of the colors/fluorophores [42–45]. The most well-known system is the Luminex xMAP, which uses 5.6-micron polystyrene spheres and has demonstrated many applications [46–53]. Such optically encoded particles are typically analyzed by flow (cyto)meters [53]. (Fig. 1). The flow (cyto)meter measures both the spectrum and/or the intensity of the colors/fluorophores which make up the code of the particle, as well as a (spectrally different) fluorescence signal at the surface of the particle (in the case of a positive reaction). Flow (cyto)meters identify individual particles at high speed [34, 54]. Particle analysis rates as high as  $10,000\text{ s}^{-1}$  are possible. By using more advanced flow (cyto)meters, not just fluorescence but also the size and the refractive index can be detected [55]. Note that particles can also be identified based on their size and refractive index (“physical encoding”).

A totally different approach is the use of light-powered  $100\text{ }\mu\text{m} \times 250\text{ }\mu\text{m} \times 250\text{ }\mu\text{m}$  microtransponders, called electronic radio frequency microchips. A serial number is stored electronically and allows the probe which is attached to the surface of a transponder to be identified. Such

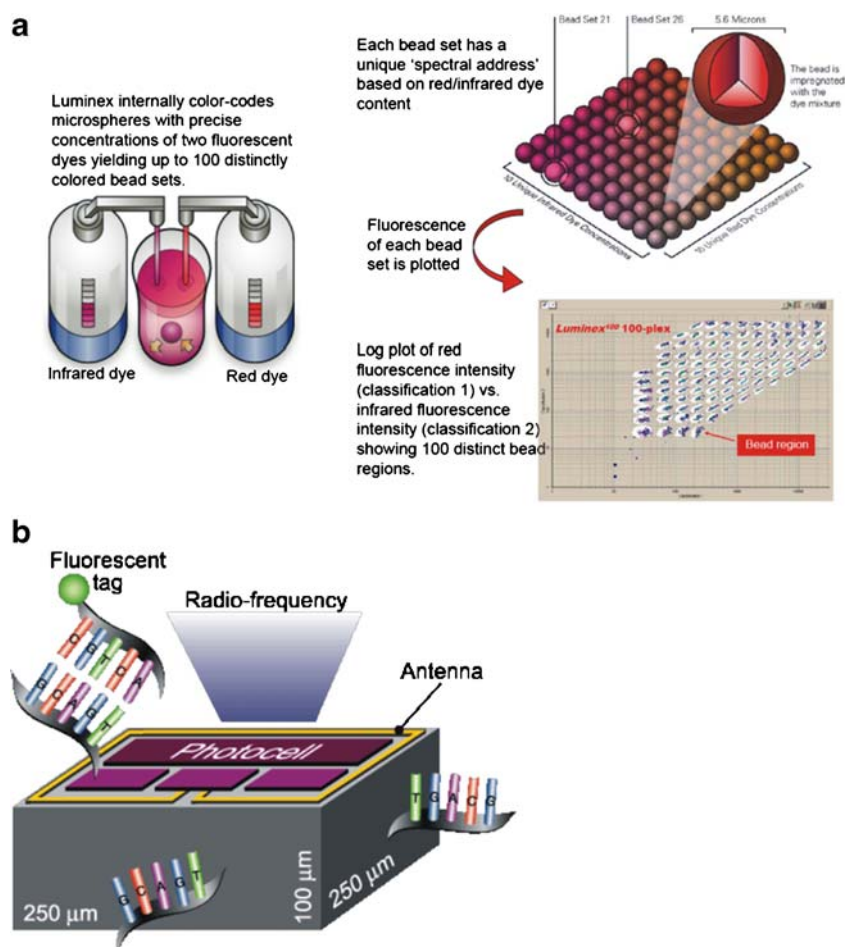
electronically encoded microcarriers are also analyzed by high-speed flow (cyto)meters modified to detect radio-frequencies [56].

A flow (cyto)meter can rapidly process optically/physically/electronically encoded particles, making it a popular reading platform for multiplexing. However, it has also several disadvantages, including: (i) its lack of portability, as flow meters are bulky; (ii) the cost (especially when multiple lasers and detectors are needed), and; (iii) the potential interference between the fluorescence from the fluorophores which make up the code and the fluorescence generated at the surface of the particles in the case of a positive reaction.

(Fluorescence) microscope platform

An alternative approach to analyzing particles is to use a (fluorescence) microscope, especially when the particles are graphically encoded. Graphically encoded particles rely on the patterning of optical elements in or at the surface of the microcarriers. As Fig. 2 explains, different graphically encoded carriers have been reported [57–66]. In contrast to optically encoded microcarriers, graphically encoded

**Fig. 1 a** The Luminex xMAP system consist of a set of 100 microspheres, each microsphere having a unique ratio of two fluorescent dyes. The microspheres are identified individually in a rapidly flowing fluid stream that passes by two laser beams: one reveals the colour code of the bead, and one quantifies the biomolecular reaction by measuring the fluorescence intensity of the reporter molecule. **b** Electronic radiofrequency microchips from PharmaSeq coated with oligonucleotide probes. Each microtransponder is an integrated circuit composed of photocells, memory, clock and antenna. The microtransponder stores information identifying the sequence of an attached oligonucleotide probe in its electronic memory. Detection occurs with a high-speed flow fluorometer modified to detect radio frequency. (a is reproduced with permission from <http://www.luminexcorp.com>, and b with permission from <http://www.pharmaseq.com>)



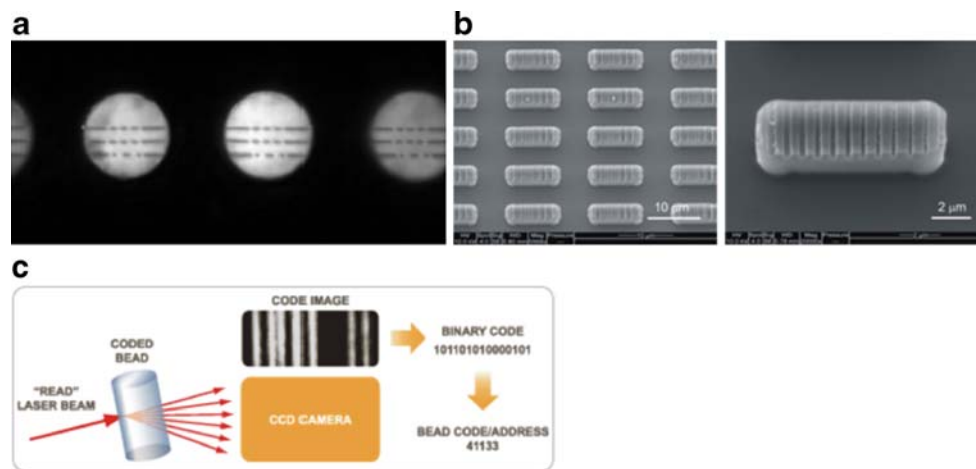


**Fig. 2** **a** Confocal fluorescent microscopy image of particles, internally barcoded by means of spatial selective photobleaching. The particles are 40  $\mu\text{m}$  in diameter. **b** SEM image of 100  $\mu\text{m}$  particles, encoded by fabrication of a nanostructured pattern on the surface; the pattern is read by detecting the spatial distribution of laser light diffracted by the tag. **c**

VeraCode, a cylindrical glass particle measuring 240 microns in length by 28 microns in diameter, inscribed with a unique digital holographic code. (**b** is reproduced with permission from ref [64], and **c** with permission from <http://www.illumina.com>)

ones are often tens to hundreds of microns in diameter or length, because the size needs to fit the “digital” code (see Fig. 2). Most of them do not use fluorescent dyes for the encoding. Hence, a broader range of fluorescence wavelengths remains available for target labeling. Graphically encoded particles often require a well-defined orientation to become accurately decoded, while some types also require

decoding at high resolution. This makes optical reading platforms (which decode the microcarriers at rest) more suitable than flow (cyto)meters (in which the carriers flow through the detection area [67]). Note that not only graphically encoded microcarriers but also the optically and physically encoded carriers described above can be analyzed by optical reading platforms. As an example, Gao

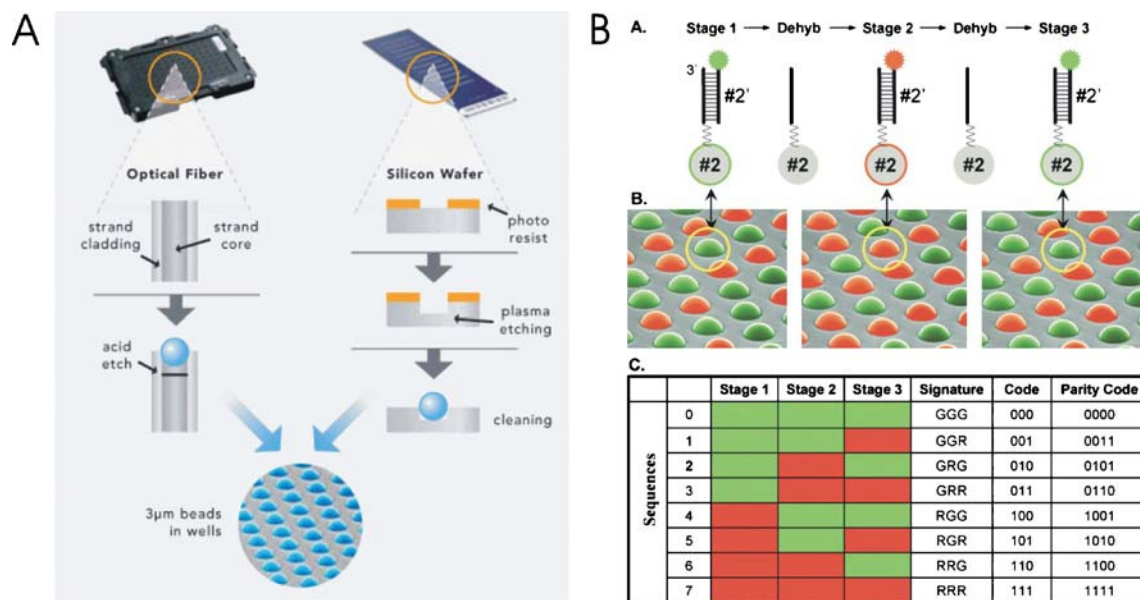


**Fig. 3** **A** Overview of the Illumina Inc. fibre-optic platform: three-micron particles self assemble in uniform microwells etched into the surface of fiber optic bundles (96-sample Array Matrix) or planar silica slides (multi-sample BeadChip). **B** Decoding process of Illumina's BeadArray technology. *Top*: schematic of the sequential hybridization process for a single particle. In stage 1, a complementary fluorescently labeled decoder oligonucleotide hybridizes to the oligonucleotide capture probe that is attached to the particle. The fluorescent signal is read by imaging the entire array. The array is then

dehybridized, and the process is repeated for two more stages. *Middle*: a scanning electron micrograph of an array of particles, artificially colored to represent three sequential hybridization stages (note that the particle circled in yellow has the color signature GRG or code 010). *Bottom*: colors are assigned to individual decoder oligonucleotides at each stage to produce a unique combination across stages. (**A** is reproduced with permission from <http://www.illumina.com> and **B** with permission from [73])

and Nie recently described the use of QD-encoded particles read out by a (conventional) optical imaging platform [44]. Note that graphically encoded microparticles have already shown potential in different application fields [60, 64, 68, 69].

#### Optical fiber platform

Illumina developed particle-based fiber optic arrays which make use of optical fiber to decode color-encoded three-micron silica particles. An optical imaging fiber consists of thousands of hexagonally packed, micrometer-sized individual optical fibres (Fig. 3) [70, 71]. By dipping the etched end of the fibre directly into the sample of encoded particles, the wells are filled with particles by self-assembly. The other end of the fiber bundle is coupled to an imaging fluorescence system that independently resolves each fiber while simultaneously viewing the entire array (Fig. 3A). Although the encoded particles are positioned in an array, their identities are known from their spectral properties [72]. To overcome some encoding limitations, recently Illumina devised a novel approach (randomly ordered DNA arrays) [73]. A different set of oligonucleotide “tag” sequences is coupled to each particle (the “code”); after self-assembling the particles on the array, the particles are decoded by sequential hybridizations with different dye-labeled decoding (complementary anti-tag) solutions (Fig. 3B) [74].

#### Multifunctionality of particles in microfluidic devices

Particles in microfluidic-based assays may have different functionalities—a particularly attractive and powerful trait—as outlined below.

*Particles offer a huge analytical surface* Clearly, when compared with flat supports, three-dimensional particles offer a huge surface which should improve the (bio) chemical reaction rates. A decade ago, Zammateo et al. demonstrated faster nucleic acid hybridization kinetics when DNA probes were coated onto the surfaces of 4.5  $\mu\text{m}$  particles instead of onto the surfaces of the wells of microtiterplates [75]. Because the microparticles continuously move in the surrounding fluid (a very dynamic process), the reactions at their surface follow “near solution” kinetics. (Spherical) microparticles also have a high surface-to-volume ratio, which enables reactions to be performed in smaller volumes without needing to resort to a smaller reaction surface. This again leads to a smaller diffusion distance and a shorter analysis time. Interestingly, even in microfluidic devices, hybridization kinetics are faster if the probes are coupled to the surface of particles

instead of the walls of the microchannels, as recently shown by Kim et al. [76]. The authors showed that the analysis of 2  $\mu\text{l}$  volumes of samples took on the order of a few minutes, with flow rates of some hundreds of nanoliters per second. Not just hybridization reactions but also protein–protein reactions take advantage of the size effect of the liquid microspace. Sato et al. demonstrated that the reaction time between antibodies and antigens coupled to the surfaces of 45- $\mu\text{m}$  polystyrene particles in a microfluidic device is 1/90 of the time needed in a conventional microtiterplate [77]. The overall analysis time was shortened from 24 h to less than 1 h, and troublesome operations could be substantially limited. It is worth mentioning that new technologies are in progress which offer high flexibility for the surface coating of microparticles, which will further broaden their molecular applications [34, 67].

*Particles allow mixing* Another advantage is that particles allow mixing, which is important for (bio)chemical reactions. Because of the dimensions, the Reynolds number of fluid flows in microfluidic devices is extremely small (usually less than 1). This means that the flow profile is laminar and that molecular transport only occurs by diffusion, which is relatively time-consuming despite the rather small dimensions involved in the assay. The lack of turbulence makes mixing in microdevices a very challenging issue. Liu et al. have shown that oscillating the sample within a microchip accelerates the hybridization of nucleic acids to their probes spotted on the bottom of the channel [78]. A factor of five improvement the signal was achieved with sample oscillation after 15 minutes of hybridization. Similar conclusions on hybridization kinetics using conventional microarrays were made by Pappaert et al.; they showed that a shear-driven flow reduces the analysis time (from 16 hours down to 30 minutes) [79]. The effect of sample oscillation could be improved even further by using microparticles which are continuously moved around in the sample to cause a local turbulent flow. This has been demonstrated by Seong et al. [80], who studied how enzymes that are immobilized on microparticles convert their substrates. Herrmann et al. recently described a microfluidic ELISA (enzyme-linked immunosorbent assay) reaction at the surfaces of microparticles, using about  $10^6$  paramagnetic particles 1  $\mu\text{m}$  in diameter trapped in a reaction chamber with dimensions of 6 mm  $\times$  2 mm  $\times$  50  $\mu\text{m}$ , and showed that mixing through the application of an external magnetic field enhances the reaction speed [81].

*Particles allow sorting* This is an important feature, as particles allow the (a) enrichment of molecules of interest from complex samples, and (b) the separation of cells, viral particles and bacteria from a large population [82].

Technical aspects related to sorting of samples with particles in microfluidics will be considered in the next section.

*Particles are very practical* Particles are also of interest from a practical point of view. For example, it is much easier to handle (detect, trap, transport) microparticles than single molecules in microfluidic systems. Also, it is much easier to modify the surfaces of microparticles than to modify the walls of a microchannel in a chip. The surfaces of microparticles can easily be modified off-chip. Adding extra probes to an existing microfluidic-based assay can be achieved by simply adding microparticles bearing the probes; it is not necessary to produce a new device. By adding more or fewer microparticles it is also straightforward to change the total capture surface (related to the number of probe molecules) in the assay (note that the total capture surface of a flat array in a microwell or microarray is constant). This can result in higher signals from particles than from flat arrays, for instance for enzyme/substrate reactions [75].

*(Encoded) particles allow multiplexing* This is highly important in situations where the amount of sample is very limited, such as in the analysis of blood from newborns, tumor tissue from biopsies, etc. Additionally, multiplexing allows more efficient and therefore less expensive use of reagents, and because the different targets are screened simultaneously they experience equal conditions at each step of the assay procedure. The integration of microparticles into microdevices for multiplexing is still in its early stage and only a few publications have demonstrated this synergism [39, 65, 83]. Technical challenges related to this integration process will be overviewed in another section.

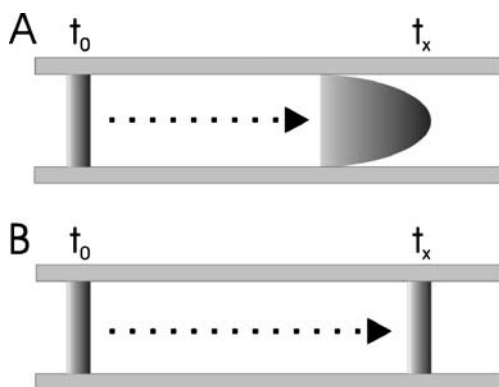


**Fig. 4** **A** Pressure-driven flow profiles at time 0 and at time  $x$  after applying pressure. After this time the profile is typically parabolic (higher velocities in the center of the channel than at the sides). **B** The electrokinetically driven flow profile stays typically pluglike after the same time (the same velocity is observed at the centre and at the sides of the channel)

## Particle trapping and sorting in microfluidics

### Propulsion of fluids in microdevices

Microfluidics involves the transport, manipulation and analysis of fluids or substances in fluids in micrometer-sized channels. Flow in microfluidics can be generated (a) mechanically (by pressure), (b) electrokinetically (electroosmotic flow; EOF), (c) by capillary forces or (d) by centrifugal forces. The type of propulsion force used is highly dependent on the application, the requested flow rate and the material composition of the microchannel.

In Fig. 4, a typical pressure-driven (e.g., caused by external syringe pumps) and electrokinetically driven flow profile is shown. The flow profile is respectively parabolic (higher flow velocities in the center than at the borders of the channel) and pluglike (equal velocities in the center and at the borders of the channel). A parabolic flow profile can be attractive for particle sorting, as will be described later. On the other hand, an EOF is preferred for microchip electrophoresis and electrochromatography, because the pluglike flow profile makes a more accurate separation possible [84, 85]. However, to enable EOF, the surfaces of the microchannels must be charged, which requires appropriate materials to fabricate the microchannels. Also, EOF requires a specific buffer solution which should be compatible with the (bio)chemical assays.

Propulsion by capillary forces, which are driven by local heating of the fluid and are due to the high heat-exchange rate in the microchannel, is still at an early stage of development and might not be compatible with (bio)chemical assaying in microfluidics, as the high temperature can have a negative effect on the assay.

Centrifugal fluidic platforms (called “lab-on-a-disc”) were recently reviewed by Madou et al. [86]. Due to the rotational speed, it is possible to have identical flow rates, to load identical volumes, and to have identical incubation times in parallel assay capillaries. Therefore, they have great potential for parallel screening [87].

### Manipulation of particles in microdevices

To perform (bio)chemical reactions on a set of particles in microfluidic devices and to take full advantage of their multifunctionality (mixing, sorting, multiplexing, etc.), they usually have to be trapped into a constrained volume inside the chip while samples and reagents are flushed through the device. Sometimes more “selective” methods are needed which aim to isolate and manipulate individual particles. For example, an excellent review on the manipulation of single cells in microfluidic devices has recently been published by Toner and Irimia [88]. Some of the methods described herein are applicable to microparticles as well.

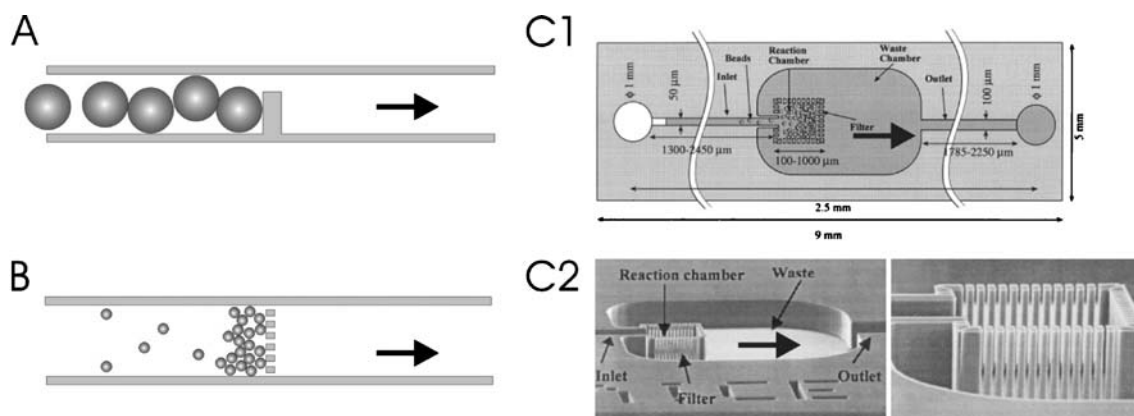


**Fig. 5** Schematics of a microchannel that contains a dam structure (A), an array of pillars aligned perpendicular to the direction of the channel (B), and a filter-chamber (C1). The arrows show the direction of the flow. SEM images of the microchip with filter-chamber as

proposed by Andersson et al. are also shown (C2). The pillars were 3  $\mu\text{m}$  wide and 50  $\mu\text{m}$  high with a spacing of 2  $\mu\text{m}$ . (C is reproduced here with permission from [90])

However, as certain microparticles have unique properties, complementary techniques for separating and sorting microparticles in microchannels exist too.

#### Mechanical trapping

The most straightforward method of trapping microparticles is through the use of a mechanical barrier. “Mechanical trapping” is only based on the size of the particles. The simplest design is a continuous flow-through microchannel that contains a dam structure (Fig. 5A) or an array of pillars aligned perpendicular to the direction of the channel and with gaps in-between the pillars that are smaller than the diameter of the particles (Fig. 5B) [77]. Different sizes of particles can be separated using mechanical barriers, but a single particle cannot be “selectively” trapped and separated [89]. Another inherent problem with mechanical trapping is clogging, especially in narrow channels. As Fig. 5C1 and C2 show, to avoid the clogging of 5.5  $\mu\text{m}$  polystyrene beads, Andersson et al. made use of a square filter chamber (side length = 100  $\mu\text{m}$ ) filled with pillars (instead of using pillars in a channel; these pillars were 3  $\mu\text{m}$  wide with a spacing of 2  $\mu\text{m}$ ) surrounded by a waste chamber [90]. Mechanical trapping of microparticles in a microdevice without clogging is also possible by microcontact printing [91], but this makes the system comparable to a microarray and thus less flexible. For the analysis of new targets, a new (microcontact-printed) device must be made.

#### Magnetic trapping

Magnetic microparticles can also be immobilized and trapped in microdevices by means of magnetic forces exerted by an external rare-earth magnet [81, 92]. The relatively large size of such an external magnet may, however, complicate the precise handling of the micro-

particles. This issue has recently been solved by using microfabricated 3-D magnetic devices positioned in a continuous flow-through microfluidic chamber (10 mm  $\times$  5 mm  $\times$  0.1 mm) [93]. Magnetic particles between 1 and 5  $\mu\text{m}$  in diameter were trapped at flow rates on the order of 10–100  $\mu\text{l}/\text{min}$ . Another original concept is the manipulation of groups of magnetic particles, as described by Rida and Gijs [94]. The local rotational motion of the particles in a microfluidic flow, generated by an external local alternating magnetic field, enhances the interaction between the particles and the liquid: 95% mixing efficiency was achieved over a mixing length of 400  $\mu\text{m}$  at flow rates on the order of 5 mm/s. However, the accurate manipulation (and separation) of individual particles by magnetic forces remains a challenge. Note that the presence of magnetic material in/on the microparticles is sometimes a limitation because it often renders them opaque.

#### Dielectrophoretic trapping

Electrically polarizable microparticles can be manipulated by dielectrophoresis (DEP) [95]. When such microparticles are subjected to an alternating electric field, a dipole moment is induced in the particles. In a nonuniform electrical field, the polarized particles experience a dielectrophoretic force which may move them to regions of high or low electrical field. The motion depends on the particle polarizability compared to the suspending medium. The magnitude and direction of the dielectrophoretic force on a particle also depends on its dielectric properties, so that a heterogeneous mixture of microparticles in a continuous flow can be spatially separated to produce a more homogeneous population in an appropriate electrical field.

The separation of microparticles by DEP in a microdevice (“DEP migration”) has been demonstrated by several research groups. Kentsch et al. developed a

particle-based assay for the detection of viruses in serum [96]. Kralj et al. simulated the flow behavior of spherical particles in a DEP-based device and verified the model for sorting differently sized particles using DEP experimentally [97]. The separation efficiency can be improved by combining DEP with other physical forces ('DEP retention'). Microparticles mechanically driven through a micro-device by pressure-based flow fields can be separated by a dielectrophoretic force perpendicular to the flow, because the particles acquire different velocities due to the parabolic flow profile, depending on their dielectric characteristics. This is an example of what is called field-flow fractionation (FFF). In FFF particles move in a flow and become separated by an external force perpendicular to the flow. Particles with different properties attain different positions relative to the chamber wall due to a number of possible forces: diffusive, hydrodynamic, gravitational (sedimentational), electrophoretic, dielectric and other forces, or a combination thereof [98, 99].

DEP forces can be used to manipulate and trap individual microparticles too. Indeed, by using micro-electrodes it is relatively easy to generate an electric field in a specific area of a microchip (the "particle trap") with physical dimensions of close to the size of the microparticles. Such "energy traps" can hold particles against volumetric fluid flow rates of about 10–50  $\mu\text{l}/\text{min}$  by forces in the sub-piconewton range [100, 101]. This technique is generally limited to trapping particles larger than approx-

imately 1  $\mu\text{m}$  because Brownian motion makes it difficult to trap smaller ones with sufficient accuracy, although some reports have described the separation of submicron particles [102]. For the trapping of multiple cells in parallel with single-cell resolution, Taff and Voldman developed a DEP trap array in which multiple cells can be sorted individually [103]. This type of device can be used for particle sorting too, and the same research group has developed an array with equal numbers of rows and columns which needs only  $2\sqrt{n}$  electrodes to control  $n$  traps (which significantly simplified fabrication) [101]. Another attractive approach that does not require patterned electrodes was demonstrated by Chiou et al. who developed a light-induced DEP trap; as Fig. 6 shows, a light image was converted into an electrical field, creating local DEP forces [104]. Each trap could be individually manipulated by programming the projected light images. The authors demonstrated the trapping of 4.5  $\mu\text{m}$  polystyrene microparticles through the parallel manipulation of 15,000 traps on a 1.3 mm  $\times$  1.0 mm area.

#### Optical trapping

A fourth way to trap particles without "physical contact" is optical trapping, which is based on the response of a dielectric microparticle to light. If a particle reflects or refracts incident laser light (with a Gaussian intensity profile), it will result in a change in the momentum of the

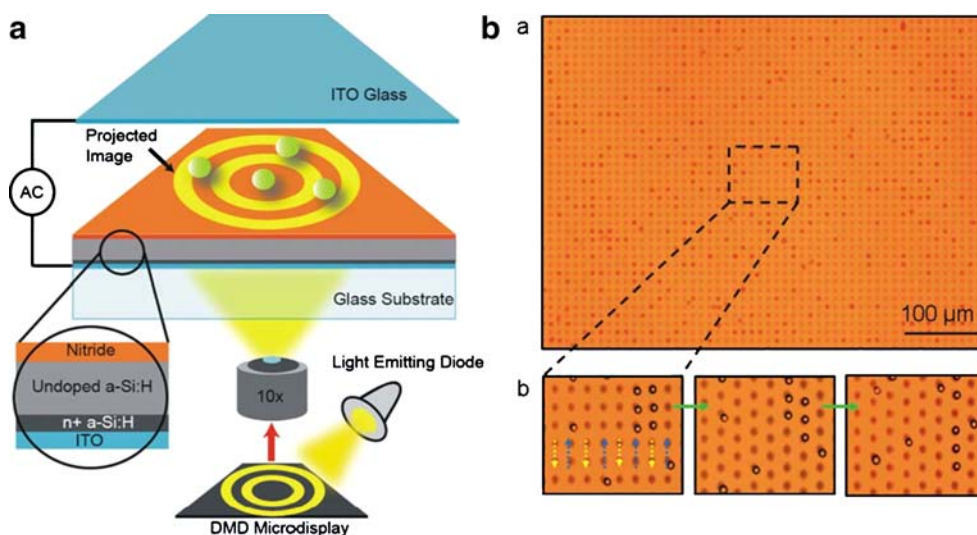


**Fig. 6** **a** Schematic overview of the microdevice used in optoelectronic tweezers (OET). Liquid that contains microscopic particles is sandwiched between the top indium tin oxide (ITO) glass and the bottom photosensitive surface consisting of ITO-coated glass covered with additional layers. The top and bottom surfaces are biased with an ac electric signal. An LED creates optical images on the digital micromirror display (DMD) which are then focused onto the photosensitive surface, resulting in a nonuniform electric field for DEP manipulation. **b** Massively parallel manipulation of single

particles by OET. *Top*: 15,000 particle traps are created across a 1.3 mm  $\times$  1.0 mm area. The 4.5- $\mu\text{m}$  sized PS particles experiencing negative DEP forces are trapped in the darker circular areas. Single-particle resolution is possible because each trap has a diameter of 4.5  $\mu\text{m}$ . *Bottom*: three snapshots from the video show the parallel transportation of single particles in part of the manipulation area. The trapped particles in two adjacent columns move in opposite directions, as indicated by the *blue* and *yellow* arrows. (Reproduced with permission from [104])



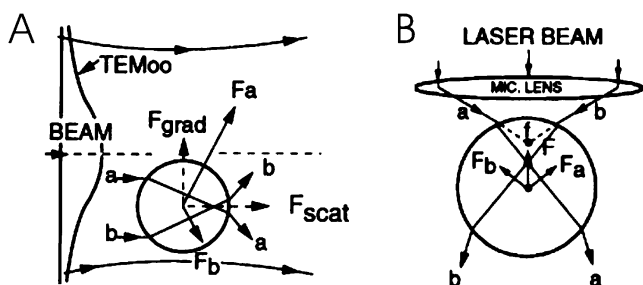


**Fig. 7** Illustration of forces that originate from radiation pressure. **A** Consider a high-index particle which is displaced from the  $TEM_{00}$  beam axis of a mildly focused Gaussian light beam. A typical pair of rays “a” and “b” striking the sphere symmetrically about its center are shown. Because most of the rays refract through the particle (resulting in a change in momentum for the light), rays “a” and “b” result in forces  $F_a$  and  $F_b$  in the direction of the momentum change, with  $F_a > F_b$  because the intensity of ray “a” is higher than that of ray “b.” By adding all such symmetrical pairs of rays striking the sphere, the resultant net force can be resolved into two components, the scattering force component ( $F_{scat}$ ) pointing in the direction of the incident light, and a gradient component ( $F_{grad}$ ) arising from the gradient in light intensity and pointing transversely toward the high-intensity region of the beam. **B** Illustration of the ray diagram of a particle trapped in an optical trap (tweezers trap). The focus of the laser ( $f$ ) is above the center of the particle, creating an upward gradient force, which is balanced by a downward scattering force (not shown), resulting in a stable laser trap. (Reproduced with permission from [106])

light (Fig. 7A). Conservation of momentum requires that the particle must undergo an equal and opposite momentum change. The manipulation of neutral microparticles by a single laser beam that is strongly focused through a high NA objective is based on the same forces of radiation pressure as depicted in Fig. 7B. In this way, the position of a single particle can be easily and accurately controlled in three dimensions, whereas in the case of DEP forces, the manipulation of the particles is limited by the fixed configuration of the electrodes in the chip. The use of so-called optical tweezers has been demonstrated by the group of Ashkin for the manipulation of individual (biological and polymeric) particles without optical damage [105, 106]. Single beam trapping can now also be done using optical fibers [107]. To trap multiple particles in parallel, efforts have been made to simultaneously generate multiple beams. However, only tens to hundreds of particles could be trapped at once [108]. A new approach to optically trapping (tens of) thousands of microparticles in a single array was recently introduced by the group of Walt. The etched fibers of an optical fiber bundle are loaded at the end with glass microparticles which act as spherical lenses. The light that is introduced via the fiber is focused by each lens, thereby creating an array of highly focused points of light [109, 110] (Fig. 8). A dense array ( $\sim 5 \times 10^4$  traps/mm<sup>2</sup> using fiber bundles with 3  $\mu$ m diameter cores) can be made in this way, from which the number of optical traps is determined by the number of fibers in the optical fiber bundle. The authors

demonstrated the trapping of 4.5  $\mu$ m sized silica particles from a particle solution with a flow rate of 3  $\mu$ m/s and calculated that each particle was trapped with approximately 12 mW of power. An attractive application of optical trapping in microdevices has been reported by Terray et al. Using optical trapping they have succeeded in arranging groups of 3- $\mu$ m silica microspheres into functional structures which could subsequently be activated to generate microfluidic valving and pumping with flow rates of about 1 nl/h [111] (Fig. 9). MacDonald et al. used a three-dimensional optical lattice to deflect selectively microparticles in a flow of mixed particles in a microdevice, while other particles were not hindered and passed straight through. The strength of the interaction between the particles and the lattice depends on their optical polarizability. A high sorting efficiency was demonstrated, even for throughputs of 25 particles per second [112].

To obtain a more precise (single particle) trapping, DEP and optical tweezing have been combined by Arai et al. They describe a device in which DEP and laser trapping forces are used to selectively isolate one single microbe from of a huge population in a microdevice in less than 20 s [113]. Laser trapping was used to trap the microbe of interest, while DEP forces were applied to exclude other

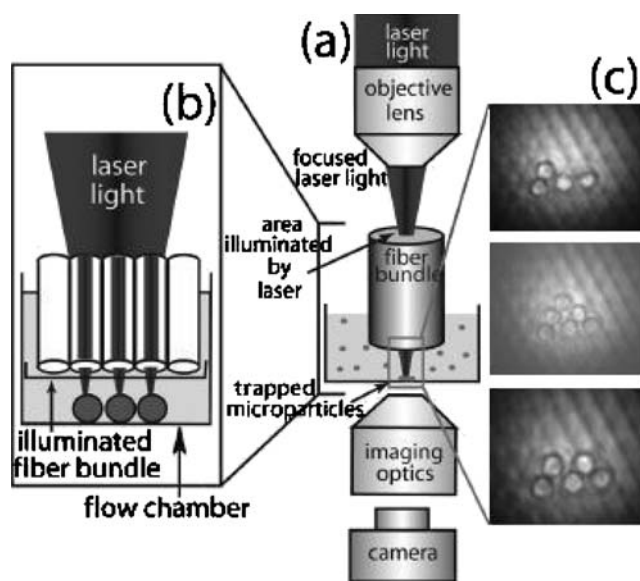


**Fig. 8** **a** Composition of an imaging fiber-based optical tweezer array system. **b** Detailed view of the region of the optical tweezer array system. Laser light illuminates a specific number of optical fibers in the array, depending on the magnification of the objective lens. All photons are continuously internally reflected on the inner walls of each fiber so that light travels down the length of the fiber. The lens elements (glass microparticles) at the end of each illuminated fiber focus the light into optical traps. Microparticles flowing into these regions become trapped by these fibers by approximately 12 mW of power (flow rate=3  $\mu$ m/s). **c** Consecutive images of trapped 4.5  $\mu$ m silica microparticles. (Reproduced with permission from [110])

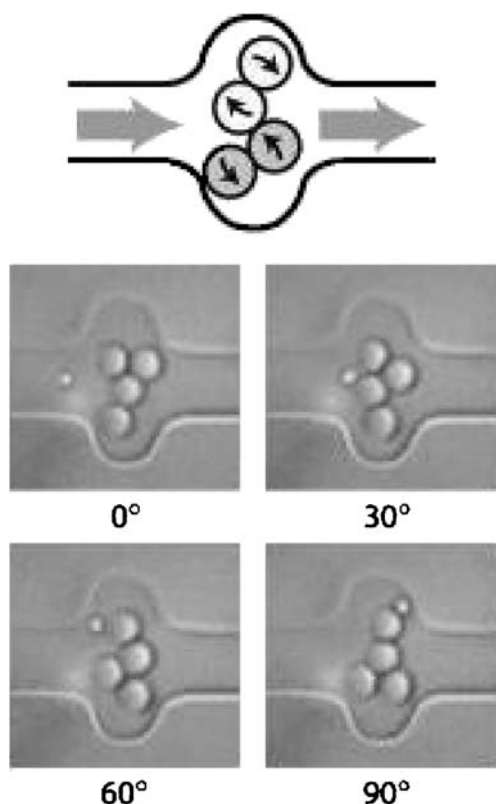


**Fig. 9** Two groups (“lobes”) of 3  $\mu\text{m}$  particles (two particles per group) are rotated in opposite directions by means of optical trapping (the top pair rotates clockwise, the bottom counterclockwise). Those functional structures are able to generate a net fluid movement from left to right. A net flow is achieved by repeated and rapid rotations, and the direction of the flow can be reversed by changing the rotation direction of the lobes. Frames are separated by two cycles to show movement of a 1.5- $\mu\text{m}$  colloidal silica tracer particle. (Reproduced with permission from [111])

objects around the target microbe. Reichle et al. combined DEP and optical tweezing (OT) for receptor–ligand interactions on single cells in microdevices [114]. Ligands were coupled to particles 4.1  $\mu\text{m}$  in diameter which were brought into contact with the cell (receptors) by OT. The latter one was held in a DEP cage.

### Integration of decoding and detection platforms

Despite the popularity of conventional flow (cyto)meters for multiplexing, it is unfortunately not straightforward to combine them with microfluidic chips; after carrying out the (bio)chemical reactions in the chip (the recipient), the particles must be transferred to the flow cytometer (which is also the case when an optical fiber platform is used), which is not desirable. Also, the flow cytometers currently available are relatively expensive, cumbersome (difficult to handle because of their size and weight), and need trained personnel.

(Fluorescent) microscope reading platforms, which allow both the (fluorescence) analysis of the (bio)chemical reaction at the particle’s surface as well as decoding, by simply placing the particle containing microfluidic device under a microscope, are of high interest. Nevertheless, some requirements need to be fulfilled for such purposes. First, the part of the microfluidic device where decoding and detection of the particles occurs should be optically transparent and compatible with the microscope optics. Besides thin glass, other materials like poly(dimethylsiloxane) (PDMS) can be used to this end [115–117]. Second, the movement of the particles must be negligible during image acquisition in the case of graphically encoded particles to avoid blurring the code. This can be accomplished by the trapping techniques described above. If the microparticles are located close to each other, parallel detection of multiple particles should be possible. The number of particles detected simultaneously will depend on the trapping system, the dimensions of the detection chamber, the field of view and the size of the particles. Thirdly, suitable dimensions should be selected for the particle detection chamber since the encoded particles have to be arranged in a monolayer. For example, Yuen et al. developed a microdevice in which glass microbarcodes can be arranged next to each other by means of centrifugal forces [118]. The device consists of a central 1-mm-high reservoir surrounded by a 35- $\mu\text{m}$ -high sorting region (less than twice the height of the 20  $\mu\text{m}$   $\times$  20  $\mu\text{m}$   $\times$  100  $\mu\text{m}$  microbarcodes). The outside of the sorting region was connected to a network of sixty 20- $\mu\text{m}$ -wide microchannels (equal to the width of the microbarcodes). After loading a suspension of the microbarcodes into the central reservoir, a monolayer of microbarcodes was formed in the sorting region by spinning the device. The microchannels stopped the microbarcodes from passing through, but acted as a drain for the liquid. The group of Ducree arranged particles in a monolayer within a disk-based detection chamber, which allowed parallel read-out of multiplexed particle-based immunoassays [39, 119].

As mentioned above, apart from microscope reading systems, other types of currently available reading instruments are not easily compatible with microfluidic devices. Microtechnology research into integrating electronics, optics, and detectors in microfluidic devices is currently ongoing. The next section overviews recent advances in this field.

### Micro flow (cyto)meter

Advances in flow (cyto)metric analysis of cells and particles in microfluidic devices have recently been described [120, 121]. Meanwhile, the first commercial microfabricated flow (cyto)meter has also become com-

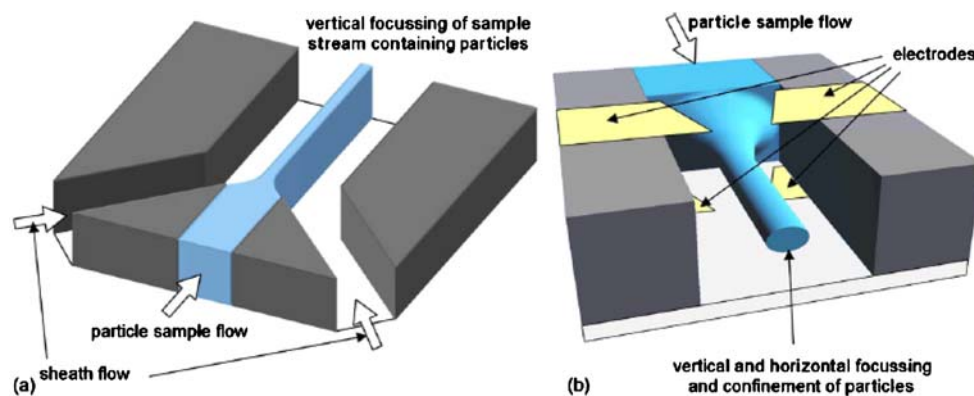


**Fig. 10** **a** Illustration of the origin of 1-D hydrodynamic focusing. The input particle stream is confined on both sides by sheath flow, resulting in a focusing of the particle stream. **b** Illustration of 2-D focusing of particles in an input sample stream by means of

dielectrophoresis. 100 nm thin microelectrodes on the top and bottom of the channel push the particles into the center of the microchannel. The electrodes do not influence the fluid flow. (Reproduced with permission from [125])

mercially available (2100 Bioanalyzer, Agilent Technologies). Similar to conventional flow meters, micro flow meters require precise fabrication to obtain optimal fluid flows in which particles are hydrodynamically focused into a single-file stream. The cost and complexity of fabricating fluidic components, traditionally made of glass, can be reduced by using inexpensive polymers like PDMS or SU-8 [122, 123]. Although sheath liquid-based hydrodynamic focusing serves as a standard technology in both conventional and micro flow (cyto)meters, it requires a large volume of sheath liquid to process a very small amount of sample (up to 1 L for 1 mL of sample), preventing further reductions in the size and volume of the whole system. It also needs continuous pumping of sheath liquid at high flow rates to generate a thin sample stream. Alternatively, ambient air can be used [124].

Another attractive approach is to use two-dimensional (2D) focusing of microparticles in a microdevice. This is illustrated in Fig. 10; in this case, Holmes et al. obtained a cylindrically focused particle sample flow (in a device 40  $\mu\text{m}$  high and 250  $\mu\text{m}$  wide) by means of dielectrophoresis (generated by 100 nm thin microelectrodes on the top and bottom of the channel) [125]. Latex particles with a diameter of 6  $\mu\text{m}$  were detected at a throughput of up to 250 particles per second. 2-D hydrodynamic focusing in a pressure-driven flow was reported by Simonnet et al. [126, 127]. They demonstrated a high-throughput microfluidic device which could analyze as many as 17,000 particles/s (particle size of 1.9  $\mu\text{m}$ ) and had a fluorescence detection accuracy comparable to those of commercial flow cytometers. Finally, focusing can also be obtained electrokinetically [128]. In 1999 Fu et al. demonstrated the basic principle of a microfabricated fluorescence-activated cell sorter, which could sort fluorescent microparticles at a throughput of approximately 10 particles per second [129]. Sorting was obtained via electrokinetic flow switching. The same sorting technique was later used by Dittrich et al.,

where sorting was preceded by reaction and detection on the same chip [115]. Meanwhile, other flow-switching techniques were introduced: hydrodynamic and valve switching [130, 131]. For more information on this, we refer the interested reader to an excellent recent review regarding  $\mu\text{FACS}$  systems written by Huh et al. [120].

#### Light-emitting diodes and detectors

In the previous section it was explained that high-throughput screening of encoded microcarriers using existing optical reading instruments is possible “on a chip,” while the optical components, such as the light source, sensors, lenses and waveguides, remain “off the chip.” Researchers have also taken on-chip high-throughput screening systems of encoded microcarriers one step further by integrating optics on the chip. The group of deMello reported thin-film polymer (polyfluorene-based) light-emitting diodes (LEDs) and thin-film organic photodiodes used as integrated excitation sources and detectors, respectively [132, 133]. Since the LED is a very small, low-power, inexpensive device, it can be integrated into microfluidics as a disposable light source. Recently, the same group made progress in the fabrication of disposable high-quality monolithically integrated optical filters [134]. Chabynic et al. reported the integration of an optical fiber and a fluorescence detector based on a microavalanche photodiode ( $\mu\text{-APD}$ ) into a microfluidic device fabricated in PDMS [135]. No transfer optics were necessary, because the pixel size of the  $\mu\text{-APD}$  matched the dimensions of the channels and the  $\mu\text{-APD}$  was incorporated in close proximity to the microchannel. However, in this system there was a lot of light loss because focusing of the LED light was not possible on the optical fiber (100  $\mu\text{m}$  diameter) that coupled light into the microdevice, resulting in ineffective illumination and insensitive analyses. This can be circumvented, as reported by Miyaki et al., by placing the light-emitting face of the

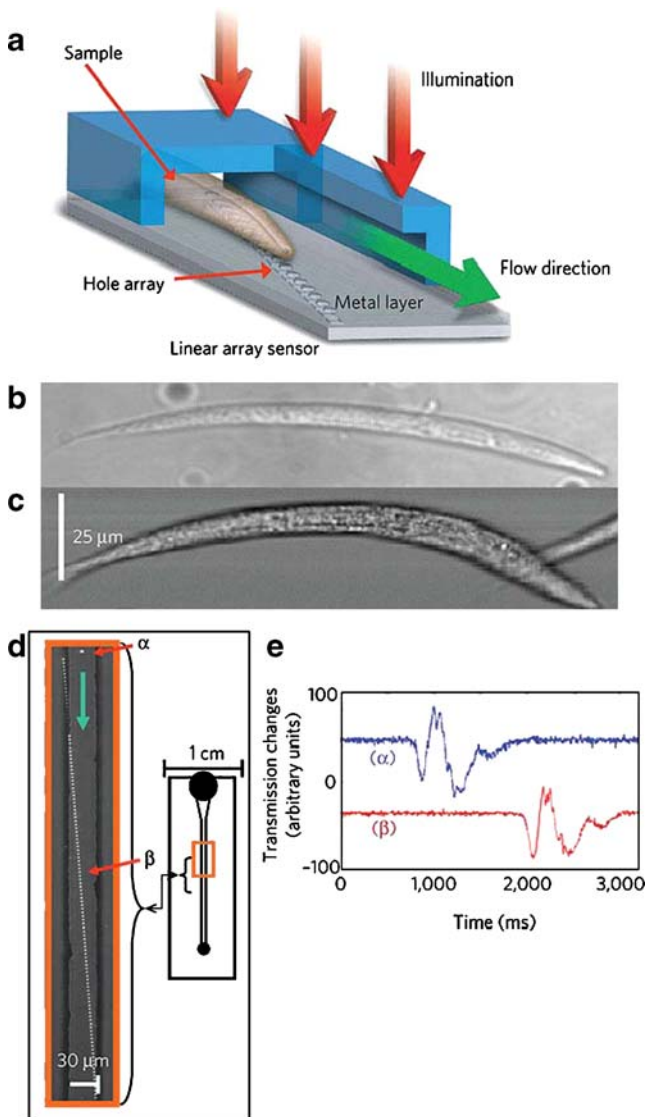


**Fig. 11** Illustration of the optofluidic microscope (OFM) integrated into a microdevice. The microfluidic channel is 15  $\mu\text{m}$  tall and 30  $\mu\text{m}$  wide. The channel is bonded onto a metal layer with an etched nano-aperture array (length=600  $\mu\text{m}$ , diameter apertures=600 nm, spacing=5  $\mu\text{m}$ ). **a** The device is uniformly illuminated from the top. The target sample flows through the channel, and the transmission through each hole is recorded on a linear array sensor (the device can be fabricated directly onto a CCD array). The composition of the transmission traces creates a transmission image of the target sample. **b** A conventional microscope image of *C. elegans* is comparable with **(c)** an optofluidic microscope image of *C. elegans*. The OFM has a measured resolution limit of  $490\pm 40$  nm. **d** By staggering the holes along the length of the channel, the separation between holes can be made equal to the pixel size of the underlying sensor array and enable the unique mapping of each hole to a pixel. The lateral displacement of the holes across the channel can be made arbitrarily small, defining the resolution of the microscope. **e** The transmission trace through two representative holes,  $\alpha$  and  $\beta$ , on the microscope as the sample flows across them. (Reproduced with permission from [138])

LED close to the microchannel by incorporating it into a chip fabricated through in situ polymerization. In this case, the detection sensitivity was comparable to that of laser-induced fluorescence [117]. Seo and Lee have reported work on a disposable integrated device with self-aligned planar microlenses for bioanalytical systems, which has LEDs as excitation sources and photodiodes as detectors [136]. The lenses enable increased detection sensitivity and reduced time for optical alignment.

### Optofluidics

In the previous section, the integration of solid state optics into microfluidic devices in order to make the device more compact was described. Meanwhile, a new field of optics has also been explored, which is called “optofluidics.” This refers to materials which are fabricated through the integration of optical components and fluids on the same chip, resulting in optical instruments that are fabricated with fluids. Lenses with a perfect curvature (a perfect spherical meniscus) can be made for instance from fluid-only devices at much lower cost than solid state optical-quality lenses. Recently, a novel microfluidic-based lensless imaging technique, termed “optofluidic microscopy” (OFM), has been reported (Fig. 11) [137, 138]. The feasibility of the method was demonstrated by imaging *C. elegans*. The acquired OFM images were comparable to those obtained with a conventional microscope (40 $\times$  objective lens). The measured resolution limit of the OFM was  $490\pm 40$  nm. A high throughput imaging rate of approximately 40 worms/min was achieved, corresponding to a sample transport rate of 300  $\mu\text{m}/\text{s}$ . Considering encoded particles of around 10  $\mu\text{m}$ , a maximal velocity of 30 particles/s can be achieved. However, as about 45% of the acquired images were rejected due to sample rotation and aggregation, the effective detection velocity will actually be much lower. Especially for graphical encoded particles, sample rotation may cause a mistake when reading out the code (e.g., by altering the diffraction pattern). In order to prevent the misinterpretation of the code, Pregibon et al. added orientation indicators to its graphically encoded fluorescently dyed particles [65]. For encoded carriers with a magnetic memory, OFM in combination with an external magnetic field could be used [67]. During imaging with the OFM, those particles can be oriented to make their codes visible by applying a weak magnetic field.

### Optical imaging fibers

Multiple articles describe the implementation of optical imaging fibers into microfluidics [117, 135]. However, the implementation of optical fiber arrays is still under

development. The group of Walt recently developed the first microfluidic platform equipped with an optical imaging fiber microarray capable of detecting DNA at the attomolar level. The use of a microfluidic platform enabled faster DNA hybridizations, lower sample volumes and 100-fold more sensitive detection when compared with a static platform (where the fiber is submerged in the target DNA sample and hybridization occurs by diffusion only); the minimal detectable concentration with the microfluidic platform was equal to 10 aM after 15 minutes of hybridization of a 50  $\mu$ l target DNA sample at flow rates of 1  $\mu$ l/min, compared with 1 pM detection with the static platform after 30 min of hybridization of a 200  $\mu$ l target DNA sample [139]. As is the case for the microscope reading platforms, future developments in order to incorporate multiplexed microparticle arrays, optics, fluidic channels and a detection unit are necessary before a portable system becomes reality.

### Conclusions and future perspectives

This review focused on miniaturized multiplexing using encoded microparticles. The combination of microfluidic technologies with encoded microparticle arrays is a very promising lab-on-a-chip tool, due to the remarkable characteristics of both technologies, which complete each other. A special emphasis was placed on the challenges of integrating current detection platforms for encoded microparticles into microdevices. The flow cytometer is currently a very popular detection platform for medium-throughput particle-based “macroscopic” multiplexing assays. When comparing the opportunities of conventional decoding instruments for miniaturized multiplexing, it seems that microscope reading platforms have a clear advantage over other platforms, because the microparticles can remain on the chip for decoding as long as the microdevice is optically transparent. Recent research shows that optical fibers may be usable “on-chip” too. However, the fiber (carrying the encoded particles) will therefore have to be inserted into a microchip in a sealed way without liquid leakage.

Work in the field of microtechnologies aimed at down-scaling the decoding unit to the microlevel, which circumvents the need to use conventional instruments for miniaturized multiplexing, is underway. Considerable cost savings can potentially be realized by integrating the optics, electronics, and detection instruments on-chip, in close proximity to the microchannels carrying the multiplexed microparticle arrays. Although this field is still in its infancy, it will probably result in new fundamental concepts for the decoding of miniaturized multiplexed microparticle assays with the same throughput as existing conventional decoding instruments, which will eventually

replace the latter ones. Promising examples are the first generation of micro flow cytometers, integrated light-emitting diodes and detectors, and so on.

Which type of detection system will become popular for multiplexing in microfluidics devices will not only depend on parameters associated with the decoding system, such as portability, costs and ease of use, but also on, for instance, the level of multiplexing that can be achieved. The latter depends on the way in which the microparticles are encoded, and is mainly defined by the intended application of the microparticle array (genotyping, protein analysis, gene expression analysis, etc.). Advances in encoding technologies of microcarriers are expected to result in new multiplexing platforms and will therefore certainly influence the future choice of detection/decoding system.

Finally, the goal of those integrated lab-on-a-chip tools is point-of-care assessment. Therefore, the real challenge will come from the coupling of the decoding modules under investigation in this study in an appropriate way on one chip to other advanced modules used for other sub-tasks, such as blood processing, extraction of DNA, RNA or proteins, and so on. In order to bring diagnostics closer to the patient, future requirements will also involve progress in non-hardware tools, like data acquisition, data management, etc. Research into each of these fields holds much promise, and we can probably expect to see the first prototypes of multiplexed particle-based LOC tools within the next decade, assuming that new nano-engineering technologies are rapidly accepted.

### References

1. Whitesides GM (2006) *Nature* 442:368–373
2. Sato K, Hibara A, Tokeshi M, Hisamoto H, Kitamori T (2003) *Anal Sci* 19:15–22
3. Figeys D, Pinto D (2000) *Anal Chem* 72:330A–335A
4. Manz A, Graber N, Widmer HM (1990) *Sens Actuators B* 1:244–248
5. Craighead H (2006) *Nature* 442:387–393
6. Gao J, Yin XF, Fang ZL (2004) *Lab Chip* 4:47–52
7. Beebe DJ, Mensing GA, Walker GM (2002) *Annu Rev Biomed Eng* 4:261–286
8. Chovan T, Guttman A (2002) *Trends Biotechnol* 20:116–122
9. Jakeway SC, de Mello AJ, Russell EL (2000) *Fresenius J Anal Chem* 366:525–539
10. deMello AJ (2006) *Nature* 442:394–402
11. Janasek D, Franzke J, Manz A (2006) *Nature* 442:374–380
12. Bange A, Halsall HB, Heineman WR (2005) *Biosens Bioelectron* 20:2488–2503
13. Hansen C, Quake SR (2003) *Curr Opin Struct Biol* 13:538–544
14. Lion N, Reymond F, Girault HH, Rossier JS (2004) *Curr Opin Biotechnol* 15:31–37
15. Tudos AJ, Besselink GJ, Schasfoort RB (2001) *Lab Chip* 1:83–95
16. Holland CA, Kiechle FL (2005) *Curr Opin Microbiol* 8:504–509

17. Verpoorte E (2002) *Electrophoresis* 23:677–712
18. Huang Y, Mather EL, Bell JL, Madou M (2002) *Anal Bioanal Chem* 372:49–65
19. Vo-Dinh T, Cullum B (2000) *Fresenius J Anal Chem* 366:540–551
20. Dupuy AM, Lehmann S, Cristol JP (2005) *Clin Chem Lab Med* 43:1291–1302
21. Walt DR (2005) *Science* 308:217–219
22. Garcia-Egido E, Spikmans V, Wong SY, Warrington BH (2003) *Lab Chip* 3:73–76
23. Dittrich PS, Manz A (2006) *Nature Rev Drug Discovery* 5:210–218
24. Haerberle S, Zengerle R (2007) *Lab Chip* 7:1094–1110
25. Situma C, Hashimoto M, Soper SA (2006) *Biomol Eng* 23:213–231
26. Sato K, Yamanaka M, Takahashi H, Tokeshi M, Kimura H, Kitamori T (2002) *Electrophoresis* 23:734–739
27. Kartalov EP, Zhong JF, Scherer A, Quake SR, Taylor CR, Anderson WF (2006) *Biotechniques* 40:85–90
28. Elshar MF, McCoy JP (2006) *Methods* 38:317–323
29. Kersten B, Wanker EE, Hoheisel JD, Angenendt P (2005) *Expert Rev Proteomics* 2:499–510
30. Ling MM, Ricks C, Lea P (2007) *Expert Rev Mol Diagn* 7:87–98
31. Lockhart DJ, Winzler EA (2000) *Nature* 405:827–836
32. Braeckmans K, De Smedt SC, Leblans M, Pauwels R, Demeester J (2002) *Nat Rev Drug Discov* 1:447–456
33. Yingyongnarongkul BE, How SE, az-Mochon JJ, Muzerelle M, Bradley M (2003) *Comb Chem High Throughput Screen* 6:577–587
34. Nolan JP, Sklar LA (2002) *Trends Biotechnol* 20:9–12
35. Wilson R, Cossins AR, Spiller DG (2006) *Angew Chem Int Ed* 45:6104–6117
36. Delehanty JB, Ligler FS (2002) *Anal Chem* 74:5681–5687
37. Bernard A, Michel B, Delamarche E (2001) *Anal Chem* 73:8–12
38. Wolf M, Juncker D, Michel B, Hunziker P, Delamarche E (2004) *Biosens Bioelectron* 19:1193–1202
39. Riegler L, Grumann M, Nann T, Riegler J, Ehlert O, Bessler W, Mittenbuehler K, Urban G, Pastewka L, Brenner T, Zengerle R, Ducree J (2006) *Sens Actuators A* 126:455–462
40. Venkatasubbarao S (2004) *Trends Biotechnol* 22:630–637
41. Wilson R, Cossins AR, Spiller DG (2006) *Angew Chem Int Ed* 45:6104–6117
42. Cook EB, Stahl JL, Lowe L, Chen R, Morgan E, Wilson J, Varro R, Chan A, Graziano FM, Barney NP (2001) *J Immunol Methods* 254:109–118
43. Fulton RJ, McDade RL, Smith PL, Kienker LJ, Kettman JR Jr (1997) *Clin Chem* 43:1749–1756
44. Gao X, Nie S (2005) *Methods Mol Biol* 303:61–71
45. Han M, Gao X, Su JZ, Nie S (2001) *Nat Biotechnol* 19:631–635
46. Dunbar SA, Jacobson JW (2000) *Clin Chem* 46:1498–1500
47. Dunbar SA, Vander Zee CA, Oliver KG, Kareem KL, Jacobson JW (2003) *J Microbiol Methods* 53:245–252
48. Dunbar SA, Jacobson JW (2005) *Methods Mol Med* 114:147–171
49. Oliver KG, Kettman JR, Fulton RJ (1998) *Clin Chem* 44:2057–2060
50. Prabhakar U, Eirikis E, Davis HM (2002) *J Immunol Methods* 260:207–218
51. Prabhakar U, Eirikis E, Miller BE, Davis HM (2005) *Methods Mol Med* 114:223–232
52. Taylor JD, Briley D, Nguyen Q, Long K, Iannone MA, Li MS, Ye F, Afshari A, Lai E, Wagner M, Chen J, Weiner MP (2001) *Biotechniques* 30:661–669
53. Vignali DA (2000) *J Immunol Methods* 243:243–255
54. Gao X, Nie S (2004) *Anal Chem* 76:2406–2410
55. Battersby BJ, Lawrie GA, Trau M (2001) *Drug Discov Today* 6: S19–S26
56. Mandecki W, Ardelt B, Coradetti T, Davidowitz H, Flint A, Huang Z, Kopacka M, Lin X, Wang Z, Darzynkiewicz Z (2006) *Cytometry A* 69:1097–1105
57. Dames A, England J, Colby E (2000) *Bio-assay technique*. WO Patent 00/16893
58. Nicewarner-Pena SR, Freeman RG, Reiss BD, He L, Pena DJ, Walton ID, Cromer R, Keating CD, Natan MJ (2001) *Science* 294:137–141
59. Penn SG, He L, Natan MJ (2003) *Curr Opin Chem Biol* 7:609–615
60. Sha MY, Walton ID, Norton SM, Taylor M, Yamanaka M, Natan MJ, Xu CJ, Drmanac S, Huang S, Borchering A, Drmanac R, Penn SG (2006) *Anal Bioanal Chem* 384:658–666
61. Walton ID, Norton SM, Balasingham A, He L, Oviso DF Jr, Gupta D, Raju PA, Natan MJ, Freeman RG (2002) *Anal Chem* 74:2240–2247
62. Braeckmans K, De Smedt SC, Roelant C, Leblans M, Pauwels R, Demeester J (2003) *Nature Mater* 2:169–173
63. Dendukuri D, Pregibon DC, Collins J, Hatton TA, Doyle PS (2006) *Nature Mater* 5:365–369
64. Banu S, Birtwell SW, Galitonov GS, Chen Y, Zheludev NI, Morgan H (2007) *J Micromech Microeng* 17:S116–S121
65. Pregibon DC, Toner M, Doyle PS (2007) *Science* 315:1393–1396
66. Zhi ZL, Morita Y, Hasan Q, Tamiya E (2003) *Anal Chem* 75:4125–4131
67. Derveaux S, Geest BG, Roelant C, Braeckmans K, Demeester J, Smedt SC (2007) *Langmuir* 23:10272–10279
68. Freeman RG, Raju PA, Norton SM, Walton ID, Smith PC, He L, Natan MJ, Sha MY, Penn SG (2005) *Methods Mol Biol* 303:73–83
69. Smith J, Onley D, Garey C, Crowther S, Cahir N, Johanson A, Painter S, Harradence G, Davis R, Swarbrick P (2005) *Ann NY Acad Sci* 1050:286–294
70. Walt DR (2000) *Science* 287:451–452
71. Epstein JR, Walt DR (2003) *Chem Soc Rev* 32:203–214
72. Michael KL, Taylor LC, Schultz SL, Walt DR (1998) *Anal Chem* 70:1242–1248
73. Gunderson KL, Kruglyak S, Graige MS, Garcia F, Kermani BG, Zhao C, Che D, Dickinson T, Wickham E, Bierle J, Doucet D, Milewski M, Yang R, Siegmund C, Haas J, Zhou L, Oliphant A, Fan JB, Barnard S, Chee MS (2004) *Genome Res* 14:870–877
74. Shen R, Fan JB, Campbell D, Chang W, Chen J, Doucet D, Yeakley J, Bibikova M, Wickham GE, McBride C, Steemers F, Garcia F, Kermani BG, Gunderson K, Oliphant A (2005) *Mutat Res* 573:70–82
75. Zammateo N, Alexandre I, Ernest I, Le L, Brancart F, Remacle J (1997) *Anal Biochem* 253:180–189
76. Kim J, Heo J, Crooks RM (2006) *Langmuir* 22:10130–10134
77. Sato K, Tokeshi M, Odake T, Kimura H, Ooi T, Nakao M, Kitamori T (2000) *Anal Chem* 72:1144–1147
78. Liu Y, Rauch CB (2003) *Anal Biochem* 317:76–84
79. Pappaert K, Vanderhoeven J, Van HP, Dutta B, Clicq D, Baron GV, Desmet G (2003) *J Chromatogr A* 1014:1–9
80. Seong GH, Crooks RM (2002) *J Am Chem Soc* 124:13360–13361
81. Herrmann M, Veres T, Tabrizian M (2006) *Lab Chip* 6:555–560
82. Horak D, Babic M, Mackova H, Benes MJ (2007) *J Sep Sci* 30:1751–1772
83. Klostranec JM, Xiang Q, Farcas GA, Lee JA, Rhee A, Lafferty EI, Perrault SD, Kain KC, Chan WC (2007) *Nano Lett* 7:2812–2818
84. Szekeley L, Guttman A (2005) *Electrophoresis* 26:4590–4604

85. Wang W, Zhou F, Zhao L, Zhang JR, Zhu JJ (2007) *J Chromatogr A* 1170:1–8
86. Madou M, Zoval J, Jia G, Kido H, Kim J, Kim N (2006) *Annu Rev Biomed Eng* 8:601–628
87. Lai S, Wang S, Luo J, Lee LJ, Yang ST, Madou MJ (2004) *Anal Chem* 76:1832–1837
88. Toner M, Irimia D (2005) *Annu Rev Biomed Eng* 7:77–103
89. Huang LR, Cox EC, Austin RH, Sturm JC (2004) *Science* 304:987–990
90. Andersson H, van der WW, Stemme G (2001) *Electrophoresis* 22:249–257
91. Andersson H, Jonsson C, Moberg C, Stemme G (2001) *Electrophoresis* 22:3876–3882
92. Fan ZH, Mangru S, Granzow R, Heaney P, Ho W, Dong Q, Kumar R (1999) *Anal Chem* 71:4851–4859
93. Ramadan Q, Samper V, Poenar DP, Yu C (2006) *Biosens Bioelectron* 21:1693–1702
94. Rida A, Gijs MA (2004) *Anal Chem* 76:6239–6246
95. Pohl HA (1978) *Dielectrophoresis*. Cambridge University Press, Cambridge
96. Kentsch J, Durr M, Schnelle T, Gradl G, Muller T, Jager M, Normann A, Stelzle M (2003) *IEE Proc Nanobiotechnol* 150:82–89
97. Kralj JG, Lis MT, Schmidt MA, Jensen KF (2006) *Anal Chem* 78:5019–5025
98. Wang XB, Vykoukal J, Becker FF, Gascoyne PR (1998) *Biophys J* 74:2689–2701
99. Pethig R, Markx GH (1997) *Trends Biotechnol* 15:426–432
100. Voldman J, Braff RA, Toner M, Gray ML, Schmidt MA (2001) *Biophys J* 80:531–541
101. Taff BM, Voldman J (2005) *Anal Chem* 77:7976–7983
102. Morgan H, Hughes MP, Green NG (1999) *Biophys J* 77:516–525
103. Voldman J, Gray ML, Toner M, Schmidt MA (2002) *Anal Chem* 74:3984–3990
104. Chiou PY, Ohta AT, Wu MC (2005) *Nature* 436:370–372
105. Ashkin A, Dziedzic JM (1987) *Science* 235:1517–1520
106. Ashkin A (1997) *Proc Natl Acad Sci USA* 94:4853–4860
107. Taguchi K, Atsuta K, Nakata T, Ikeda M (2001) *Opt Quantum Electron* 33:99–106
108. Daria VR, Rodrigo PJ, Gluckstad J (2004) *Biosens Bioelectron* 19:1439–1444
109. Tam JM, Biran I, Walt DR (2006) *Appl Phys Lett* 89:194101
110. Tam JM, Biran I, Walt DR (2004) *Appl Phys Lett* 84:4289–4291
111. Terray A, Oakey J, Marr DW (2002) *Science* 296:1841–1844
112. MacDonald MP, Spalding GC, Dholakia K (2003) *Nature* 426:421–424
113. Arai F, Ichikawa A, Ogawa M, Fukuda T, Horio K, Itoigawa K (2001) *Electrophoresis* 22:283–288
114. Reichle C, Sparbier K, Muller T, Schnelle T, Walden P, Fuhr G (2001) *Electrophoresis* 22:272–282
115. Dittrich PS, Schwille P (2003) *Anal Chem* 75:5767–5774
116. Gambin Y, Legrand O, Quake SR (2006) *Appl Phys Lett* 88:174102
117. Miyaki K, Guo YL, Shimosaka T, Nakagama T, Nakajima H, Uchiyama K (2005) *Anal Bioanal Chem* 382:810–816
118. Yuen PK, Despa M, Li CC, Dejneka MJ (2003) *Lab Chip* 3:198–201
119. Grumann M, Dobmeier M, Schippers P, Brenner T, Kuhn C, Fritsche M, Zengerle R, Ducrece J (2004) *Lab Chip* 4:209–213
120. Huh D, Gu W, Kamotani Y, Grotberg JB, Takayama S (2005) *Physiol Meas* 26:R73–R98
121. Holmes D, She JK, Roach PL, Morgan H (2007) *Lab Chip* 7:1048–1056
122. McDonald JC, Duffy DC, Anderson JR, Chiu DT, Wu H, Schueller OJ, Whitesides GM (2000) *Electrophoresis* 21:27–40
123. Wang Z, El-Ali J, Engelund M, Gotsaed T, Perch-Nielsen IR, Mogensen KB, Snakenborg D, Kutter JP, Wolff A (2004) *Lab Chip* 4:372–377
124. Huh D, Tkaczyk AH, Bahng JH, Chang Y, Wei HH, Grotberg JB, Kim CJ, Kurabayashi K, Takayama S (2003) *J Am Chem Soc* 125:14678–14679
125. Holmes D, Morgan H, Green NG (2006) *Biosens Bioelectron* 21:1621–1630
126. Simonnet C, Groisman A (2005) *Appl Phys Lett* 87:114104
127. Simonnet C, Groisman A (2006) *Anal Chem* 78:5653–5663
128. McClain MA, Culbertson CT, Jacobson SC, Ramsey JM (2001) *Anal Chem* 73:5334–5338
129. Fu AY, Spence C, Scherer A, Arnold FH, Quake SR (1999) *Nat Biotechnol* 17:1109–1111
130. Kruger J, Singh K, O'Neill A, Jackson C, Morrison A, O'Brien P (2002) *J Micromech Microeng* 12:486–494
131. Wolff A, Perch-Nielsen IR, Larsen UD, Friis P, Goranovic G, Poulsen CR, Kutter JP, Telleman P (2003) *Lab Chip* 3:22–27
132. Hofmann O, Miller P, Sullivan P, Jones TS, deMello JC, Bradley DDC, deMello AJ (2005) *Sens Actuators B* 106:878–884
133. Edel JB, Beard NP, Hofmann O, deMello JC, Bradley DD, deMello AJ (2004) *Lab Chip* 4:136–140
134. Hofmann O, Wang X, Comwell A, Beecher S, Raja A, Bradley DD, deMello AJ, deMello JC (2006) *Lab Chip* 6:981–987
135. Chabinyc ML, Chiu DT, McDonald JC, Stroock AD, Christian JF, Karger AM, Whitesides GM (2001) *Anal Chem* 73:4491–4498
136. Seo J, Lee LP (2004) *Sens Actuators B* 99:615–622
137. Heng X, Erickson D, Baugh LR, Yaqoob Z, Sternberg PW, Psaltis D, Yang C (2006) *Lab Chip* 6:1274–1276
138. Psaltis D, Quake SR, Yang C (2006) *Nature* 442:381–386
139. Bowden M, Song LN, Walt DR (2005) *Anal Chem* 77:5583–5588